

# Toward a Surgeon-in-the-Loop Ophthalmic Robotic Apprentice using Reinforcement and Imitation Learning

Amr Gomaa\*, Bilal Mahdy\*, Niko Kleer\* and Antonio Krüger\*

**Abstract**—Robotic-assisted surgical systems have demonstrated significant potential in enhancing surgical precision and minimizing human errors. However, existing systems lack the ability to accommodate the unique preferences and requirements of individual surgeons. Additionally, they primarily focus on general surgeries (e.g., laparoscopy) and are not suitable for highly precise microsurgeries, such as ophthalmic procedures. Thus, we propose a simulation-based image-guided approach for surgeon-centered autonomous agents that can adapt to the individual surgeon’s skill level and preferred surgical techniques during ophthalmic cataract surgery. Our approach utilizes a simulated environment to train reinforcement and imitation learning agents guided by image data to perform all tasks of the incision phase of cataract surgery. By integrating the surgeon’s actions and preferences into the training process with the surgeon-in-the-loop, our approach enables the robot to implicitly learn and adapt to the individual surgeon’s unique approach through demonstrations. This results in a more intuitive and personalized surgical experience for the surgeon. Simultaneously, it ensures consistent performance for the autonomous robotic apprentice. We define and evaluate the effectiveness of our approach using our proposed metrics; and highlight the trade-off between a generic agent and a surgeon-centered adapted agent. Moreover, our approach has the potential to extend to other ophthalmic surgical procedures, opening the door to a new generation of surgeon-in-the-loop autonomous surgical robots. We provide an open-source simulation framework for future development and reproducibility.

## I. INTRODUCTION

Several decades ago, surgical robots were considered implausible and unachievable; however, the da Vinci Surgical Robotic System [1] has been assisting surgeons to perform millions of operations over the past decade [2]. Similarly, with the current advancement in artificial intelligence and machine learning, autonomous surgical robots could be a plausible, feasible, and achievable concept. In a review by Datta et al. [3], it was shown that reinforcement learning (RL) has been a cornerstone for the automation of surgical robots for the last decade. Although some of the existing tools bridge the gap between reinforcement learning algorithms and robotic surgery simulations, such as dVRL [4], methodologies that are concluded with positive results usually restrict the use case to a specific narrowed part of the surgical environment. In their review, Datta et al. [3] limit the scope of reinforcement learning scenarios to auxiliary tasks within surgical protocols, such as determination of intravenous (IV) dosage or patient-assisted ventilation monitoring. However, more physically interactive applications often

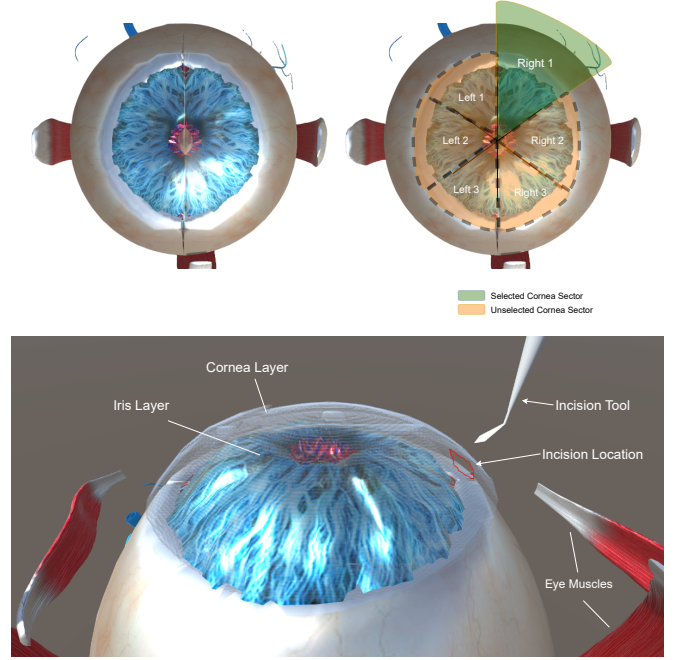


Fig. 1: Our cataract surgery simulation model. Top: Cornea illustrative sectorization for personalized approach modeling. Bottom: The surgical tool performing an incision in the cornea (highlighted in red).

face limitations when the environment becomes too complex for the agent to navigate. Bourdillon et al. [5] combined RL in a virtual robotic surgery simulation environment to train a proximal policy optimization (PPO) agent to operate a pair of scissors on a tissue-like object. The reliability of the results was positive when motion was restricted to a single axis, but dropped significantly when more than one was introduced. Other applications of reinforcement learning in surgical procedures such as [6], [7], [8], [9], [10], [11], [12] are also similarly bound by complexity constraints or limited function.

In addition to enhancing surgical precision and patient safety, there is growing interest in the integration of advanced technologies, such as surgical robots, into the field of cataract surgery [13] (see Fig. 1). The potential of combining imitation learning with robotic assistance holds great promise for revolutionizing the surgical landscape. Although in this work we primarily consider improving surgical techniques through imitation learning in a simulated environment, we also highlight the future prospect of transferring the acquired

\*All authors are with the German Research Center for Artificial Intelligence (DFKI) and Saarland Informatics Campus, Saarland University, 66123 Saarbrücken, Germany `firstName.lastName@dfki.de`

knowledge and skills to a physical surgical robot. In other words, by pretraining an imitation learning agent to perform cataract surgery with increased precision within a simulation environment, we provide a base model for the seamless transfer of these skills to a physical robotic surgical system through Transfer Learning [14]. This integration of robotic assistance into surgery can further amplify surgical precision, minimize human error, and allow highly controlled and precise surgical maneuvers [15]. By exploring the correlation and trade-off between imitation learning, virtual simulation, and robotic assistance, our research aims to improve the outcome of cataract surgery by improving surgical precision and reducing surgeon errors through the utilization of autonomous and semi-autonomous surgical robots.

In summary, our **contributions** are threefold, as follows.

- 1) We propose a novel approach for customizing the surgical behaviour of an imitation learning agent based on visual input and recorded demonstrations, tailoring it to individual surgeon techniques through *Transfer Learning* techniques.
- 2) We introduce an innovative 3D simulation framework in Unity, encompassing a precise and appropriately scaled model of the human eye, a set of scaled microsurgery tools, and a cohesive implementation of incision/collision physics that govern interactions between the tools and different eye components
- 3) We investigate and evaluate an incision experiment using our approach and our environment and demonstrated an agent adept at executing the incision phase of an ophthalmic cataract surgery

## II. BACKGROUND AND RELATED WORK

### A. Automation of Surgical Robots

Surgery, as a medical specialty, uses operative manual and instrumental techniques applied to the human body to treat a patient's injury or pathological condition. Such microscopic procedures are performed manually by experienced surgeons with the help of a surgical microscope and require, in addition to trained hand-eye coordination and the planned procedure, machines and technology to make time-critical and risky interventions feasible. Surgical robotic imaging microscopes are currently manually configured by the operating surgeon to ensure optimal support through the imaging properties of the visual device directed at the surgical zone. However, imaging requirements in terms of positioning, viewing, and focus plane may change throughout the operation, making it necessary for surgeons to adapt the configuration of the surgical microscope. Since adjustments must be performed manually, a short-term interruption of the operation becomes necessary. Individual risk considerations are made in each case as to whether visual section correction is effective in the present surgical situation, which could negatively affect the outcome of the surgery if taken incorrectly. Hence, there have been recent advances in the hand-free configuration of the microscope, such as mouth-controlled joysticks or foot control with the help of pedals [16], [17],

[18]. However, these approaches are impractical and allow too few degrees of freedom to meet the complex requirements for the various settings of the microscopic frame.

### B. Reinforcement Learning (RL)

RL dates back to 1983 when it was first introduced in the research areas of cybernetics, statistics, psychology, and neuroscience [19], [20]. In 1996, Kaelbling et al. [19] highlighted the use of RL in artificial intelligence (AI) research as a way of teaching an agent how to complete a task based only on reward and punishment (i.e., without specifying how the task is actually achieved). With recent advances in computational power, researchers were able to combine RL with deep learning approaches and apply these algorithms to specific tasks with a predefined reward system (e.g., Atari games [21]).

There are different types of reinforcement learning algorithms commonly used, each with its own characteristics and applications. One type is value-based methods, where the agent learns to estimate the value of different states or state-action pairs. These algorithms, such as Q-learning [22] and deep Q-Networks (DQN) [21], aim to find an optimal value function that guides the agent's decision-making. Another type is policy-based methods, which directly learn a policy, a mapping from states to actions. These algorithms, including REINFORCE [23] and Proximal Policy Optimization (PPO) [24], explore the policy space and optimize the agent's policy to maximize the expected cumulative rewards.

However, due to the computationally expensive nature of RL, researchers were unable to apply such algorithms to complex tasks. Additionally, current advances in the RL approach depend on hand-crafted sensitive, unstable reward systems that require high computational power and extended training time. Therefore, the need for a reward-free RL algorithm increased.

### C. Imitation Learning

One of the methodologies used to solve the dilemma of defining the reward function with RL is imitation learning. Also known as learning from demonstrations, it is a subfield of machine learning that focuses on training agents to mimic expert behavior. Unlike reinforcement learning, where agents learn through trial and error, imitation learning uses expert demonstrations as a source of guidance. In this approach, an agent learns a policy by observing and mimicking the actions performed by human or expert demonstrators. By learning from preexisting knowledge and demonstrations, imitation learning offers several advantages, such as faster convergence and improved sample efficiency compared to pure reinforcement learning [25], [26]. It finds applications in various domains, including robotics [27], [28], [29], [30], autonomous driving [31], [32], [33], and virtual simulation [34]. Imitation learning algorithms, such as Behavioral Cloning [35], Inverse Reinforcement Learning (IRL) [36], and Generative Adversarial Imitation Learning (GAIL) [37], provide frameworks for effectively transfer expert knowledge to autonomous agents. However, imitation learning also faces

challenges such as handling distribution shift between expert demonstrations and agent exploration, generalization to novel situations, and addressing the trade-off between imitation accuracy and exploration for robust decision making [25]. Researchers continue to advance imitation learning techniques to address these challenges and enhance the ability to learn from expert demonstrations.

#### D. Ophthalmic Cataract Surgery

Cataract surgery is a common surgical procedure performed to treat cataracts, a condition characterized by clouding of the natural lens of the eye [38]. During surgery, the clouded lens is removed and replaced with an artificial intraocular lens (IOL). The procedure is generally performed under local anesthesia and, in some cases, with mild sedation [39]. Surgeons make a small incision in the cornea, the transparent outer layer of the eye, and access the clouded lens. Through various techniques, such as phacoemulsification [40], the surgeon breaks down and removes cloudy lens fragments. Once the lens is completely removed, an IOL is inserted into the eye to restore clear vision. Cataract surgery is known for its high success rate and relatively quick recovery period, allowing individuals to regain improved vision and resume daily activities with minimal disruption.

### III. METHODOLOGY

The methodology presented in this paper outlines an innovative approach to training an imitation learning agent capable of performing the cataract surgery incision task within a customized Unity simulation environment. To augment surgical training and improve surgical outcomes, we propose a comprehensive framework that uses state-of-the-art techniques in reinforcement learning and imitation learning. By combining expert demonstrations, policy optimization algorithms, and a realistic surgical simulator, our methodology empowers the agent to learn complex surgical maneuvers, decision-making processes, and delicate interactions with surgical tools. This section details the key components of our approach, including data collection, pre-processing, training pipeline, simulation environment design, and performance evaluation metrics.

#### A. Simulation Environment

The simulation environment utilized in this study serves as a vital component of our training methodology, providing a realistic and immersive platform for the imitation learning agent to develop surgical skills. Specifically designed for cataract surgery, the simulation environment incorporates meticulously modeled surgical tools (provided by [41], see Fig. 2), a highly accurate human eye model (see Fig. 1), and a three point-of-view camera system (see Fig. 4). The primary incision tool, a 2.75mm Keratome Ophthalmic Knife (shown in Fig. 2), is intricately modeled to capture the physical properties and functionalities of the real tool. Furthermore, to ensure precise interactions and realistic dynamics, the model of the eye incorporates an extensive collision-physics engine. This physics engine accurately simulates the delicate

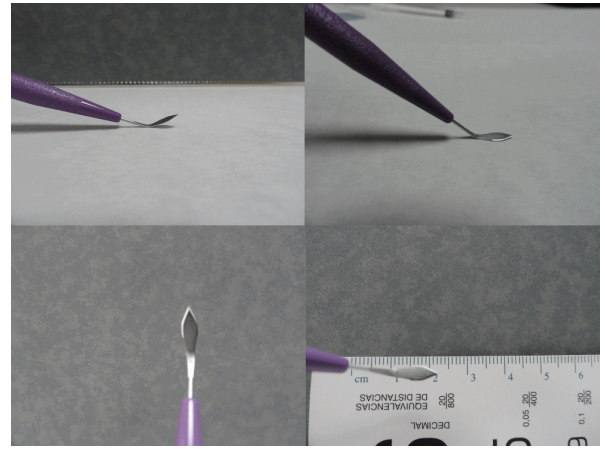


Fig. 2: A 2.75mm Keratome Ophthalmic Knife mapped and digitalized in 3D by [41].

interactions between surgical tools and ocular tissues by dynamically removing parts of the mesh corresponding to the tool edge’s location and alignment. This demonstrates precise control and an open sandbox environment for the agent to explore and learn.

The eye model used in this study comprises a comprehensive representation of its various anatomical components, including the cornea, iris, veins, arteries, and optic nerves. Each component is meticulously modeled to capture its unique characteristics and structural intricacies. The cornea, which acts as the transparent outermost layer, is faithfully reconstructed to emulate its curved shape and refractive properties. The iris, responsible for regulating the amount of light entering the eye, is accurately depicted with its intricate patterns and radial muscle fibers. Voxelization techniques were employed to discretize the eye model into a three-dimensional grid, with each voxel measuring 0.01mm in size. This high resolution voxelization enables precise simulations of surgical procedures, such as cutting or incisions, and ensures accurate modeling of tissue interactions. The veins, arteries, and optic nerves, crucial for the eye’s vascular supply and visual information transmission, are intricately represented to mimic their branching networks and connectivity within the eye. By incorporating these detailed submodels and employing voxelization techniques, our eye model provides a realistic and fine-grained simulation environment, enabling the agent to simulate and learn from intricate surgical maneuvers within the eye with a high degree of fidelity.

#### B. Agent Architecture

In our approach, the agent architecture combines elements from traditional reinforcement learning, GAIL, and PPO.

1) *Low Poly*: Our agent performs preliminary training in a significantly less complex environment, including an eye model with a low polygon count, no textures, lower degrees of freedom in tool manipulation and a more lenient reward function. This acts as a stepping stone to facilitate convergence in the high poly environment. The reward

function is designed so that the agent is simply rewarded for performing an incision anywhere on the cornea layer without conforming to a particular surgery technique and without brushing, cutting, or damaging another part of the eye anatomy in any way possible. Skipping this pre-training results in the agent being unable to learn the simulation environment’s complexity. As seen in Fig. 3, the agent trained using traditional RL in the low poly environment can converge steadily and consistently. In contrast, the agent trained directly in the high poly environment cannot capture the visual complexity throughout the training process.

2) *High Poly*: After the agent converges in the low poly environment, it is transferred to the higher poly environment and tuned to learn its new rules. The high poly environment rewards the agent using the same conditions as the low poly environment. However, it contributes three additions as follows. A highly textured eye model with high polygon counts, a punishment for the agent if it delays the incision, and a punishment for the agent if it performs an incision that does not conform to proper cataract surgery techniques or could cause complications for the patient [42].

### C. Training Pipeline

We employ the pre-trained agent as a foundational benchmark for training various agents, each with distinct reward ratios comprising a blend of GAIL and standard RL rewards. These reward ratios are denoted as strength factors  $\lambda_{gail}$  and  $\lambda_{env}$ , which are used to scale the rewards generated by their respective algorithms. The total reward for each agent is subsequently calculated as the weighted sum of these individual rewards. Algorithm 1 shows the fine-tuning procedure for the adapted agents. Table I highlights the specific ratios of  $\lambda_{gail}:\lambda_{env}$  applied to the fine-tuned agents.

### D. Action, Spatial, and State Space Representations

The action space, state space, and spatial representation play a crucial role in enabling the agent to interact effectively within the simulation environment of cataract surgery. The agent is equipped with a 3D Cartesian coordinate-based

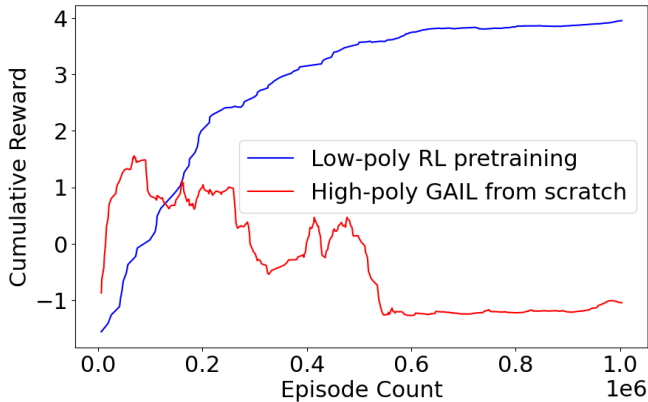


Fig. 3: Cumulative reward convergence using RL pretraining on a low-poly eye model versus using a GAIL agent directly on a high-poly eye model.

### Algorithm 1 Cataract Surgery Adapted GAIL Agent

---

**Require:** Expert Observation-Action pairs  $(O_E, A_E)$ , Pre-trained policy  $\pi_0$ , Reward function  $env(o, a)$ , GAIL discriminator  $D(o, a)$ , GAIL strength factor  $\lambda_{gail}$ , Environment reward strength factor  $\lambda_{env}$

**Ensure:** Optimized agent policy  $\pi^*$

```

for  $t = 0, 1, 2, \dots, T$  do
    Sample action  $a_t$  from policy  $\pi_0$  and observation  $o_t$ 
     $r_{env_t} = env(o_t, a_t)$  ▷ Environment Reward
     $r_{gail_t} = D(o_t, a_t | O_E, A_E)$  ▷ GAIL Reward
     $r_{total_t} = r_{gail_t} \lambda_{gail} + r_{env_t} \lambda_{env}$ 
    Use PPO to optimize agent  $\pi^*$  using reward  $r_{total_t}$ 
end for
return  $\pi^*$ 

```

---

TABLE I: Strength factors for GAIL and RL rewards for each fine-tuned agent.

	Strength Factor	
Agent	$\lambda_{gail}$	$\lambda_{env}$
NonAdaptAgent	0.0	1.0
BalancedAdaptAgent	0.5	0.5
HighAdaptAgent	0.7	0.3
PurelyAdaptAgent	1.0	0.0

action space, allowing precise manipulation of the incision tool in the simulated environment. This provides the agent with the ability to perform intricate movements and precisely control the position and orientation of the tool during the surgical procedure.

In terms of state space, the agent gathers visual observations from three different cameras strategically positioned for optimal visual coverage. Additionally, the agent receives information about the exact position of the incision tool, enabling it to have real-time awareness of its own location within the simulation. Furthermore, the agent’s observations include the Euclidean distance between the tip of the tool and the eye model, offering valuable insight into the proximity and potential contact between the tool and the eye.

**Surgical Vision:** The three cameras capture a top view, an upper side view, and an upper corner view, providing a comprehensive perspective of the surgical scene (shown in Fig. 4). These observations are obtained as colored pixel data with a resolution of  $128 \times 128 \times 3$ , allowing the agent to perceive fine details and spatial relationships between different elements in the environment.

## IV. RESULTS AND DISCUSSION

The experimental setup aimed to develop a personalized model that could adapt to the individual approach of a surgeon during cataract surgery. To emulate this personalized adaptation, the cornea was divided into sectors, representing distinct regions of the surgical site. Expert demonstrations



were recorded for each sector, capturing the specific techniques and approaches of individual surgeons. By training the imitation learning agent on these sector-specific demonstrations, our motivation was to create a model that could learn and emulate the unique approach and expertise of an individual surgeon. This personalized approach aimed to improve surgical precision by allowing the agent to adapt its policy to match the surgeon’s preferences and techniques in each sector of the cornea.

#### A. Performance Metrics

For this experiment, we introduce two main metrics for measuring performance: *Surgery Completion Rate (SCR)* and *Adaptive Surgery Success Rate (AdSSR)*. The former defines the rate at which the agent can complete an incision without damaging any part of the eye model while also conforming to proper cataract surgery techniques or could present complications to the patient [42]. The latter defines the rate at which the agent is able to follow the correct technique demonstrated by the expert surgeon when performing the incision.

#### B. Simulated Scenarios

To evaluate the adaptive agent’s capacity to emulate the surgical style of a chosen surgeon, we conducted experiments across varying levels of sector resolution. In the lower sector resolution tests, we assessed the agent’s capability to execute incisions on either the left or right half of the eye (i.e., two sector resolution), guided by an expert surgeon demonstrating these respective incisions. On the contrary, the higher sector resolution experiment further divides each half into three distinct sectors, resulting in a total of six sectors denoted as *Left 1 to 3* and *Right 1 to 3* as shown in Fig. 1). Note that the sectors are not exactly uniform to nonsymmetry in the eye model. Thus, left and right sectors are not exactly halves, but they have a ratio of one to three respectively,

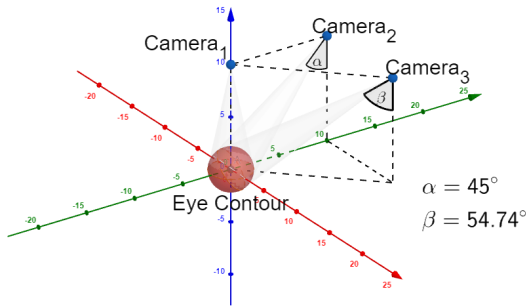


Fig. 4: Camera setup for comprehensive surgical scene perception. The top-view camera (Camera 1) provides an overhead vantage point, capturing the surgical field and the overall context. The upper-side view camera (Camera 2) offers a lateral perspective, enabling observation of side-specific details and depth perception. Lastly, the camera with a view in the upper corner (Camera 3) provides an angled viewpoint, enhancing spatial awareness and facilitating precise tool manipulation.

i.e., random chance levels for hitting left and right sectors are 25% and 75%, respectively.

1) *From Pre-training to Adapting*: As explained in section III-B, a pretraining operation was implemented before adapting each agent to the approach of a particular surgeon. The pretraining phase encompassed 5M episodes, which was subsequently succeeded by an adaptation phase consisting of 500k episodes. Fig. 5 highlights the behavior of each agent during the adaptation phase to gain insight into the modification of the strength factors shown in Table I. It is shown that the SCR of an agent consistently decreases with the higher ratio of  $\lambda_{gail}$  to  $\lambda_{env}$  ending at 0.835 with the *PurelyAdaptAgent* from the 0.994 of the *NonAdaptAgent*. This shows that the more the agent tries to mimic the expert surgeon, the less likely it is to successfully complete the surgical incision. However, this is an expected trade-off for obtaining an adaptive agent that is in accordance with a particular surgeon’s approach.

2) *Adaptive Performance*: Although SCR decreases with incentivized adaptation, the opposite effect can be observed for our second metric. Table II shows a clear and significant increase in AdSSR with higher values of  $\lambda_{gail}$  compared to  $\lambda_{env}$ . The agent adapted to the left incision approach shows an increase in AdSSR of 150% of its original value, while the agent adapted to the right incision approach shows an increase of 16.6%. This imbalance can be explained by the originally skewed AdSSR of the *NonAdaptAgent* being 28% and 72% for left and right, respectively.

However, even the smaller increase of 16.6% of the right incision approach surpasses the maximum decrease of the SCR value, which is 16%. This indicates that while the approach may impact the agent’s proficiency in executing surgical incisions, it significantly enhances the adaptability indicator at a faster pace. This contrast can be seen for the left and right incision approaches in Fig. 6.

#### V. CONCLUSION AND FUTURE WORK

In conclusion, this work introduces an innovative approach to enhance the precision and adaptability of autonomous surgical agents, particularly in the context of ophthalmic cataract surgery. The proposed method utilizes a simulated environment combined with reinforcement and imitation learning techniques to train agents capable of performing the intricate incision phase of cataract surgery. Additionally, we laid the groundwork for several exciting avenues of future work. First, our work paves the way for online real-time learning, allowing autonomous agents to continuously adapt and refine their skills based on live demonstrations from surgeons. This approach allows agents to stay up-to-date with evolving surgical techniques and adapt to specific situations. Second, transitioning from simulation environments to physical robots operating on synthetic porcine eyes represents a crucial step towards practical implementation in clinical settings. The development of tangible robotic systems capable of replicating the adaptability demonstrated in this work could have a significant impact on the field of ophthalmic surgery. Furthermore, future work involves

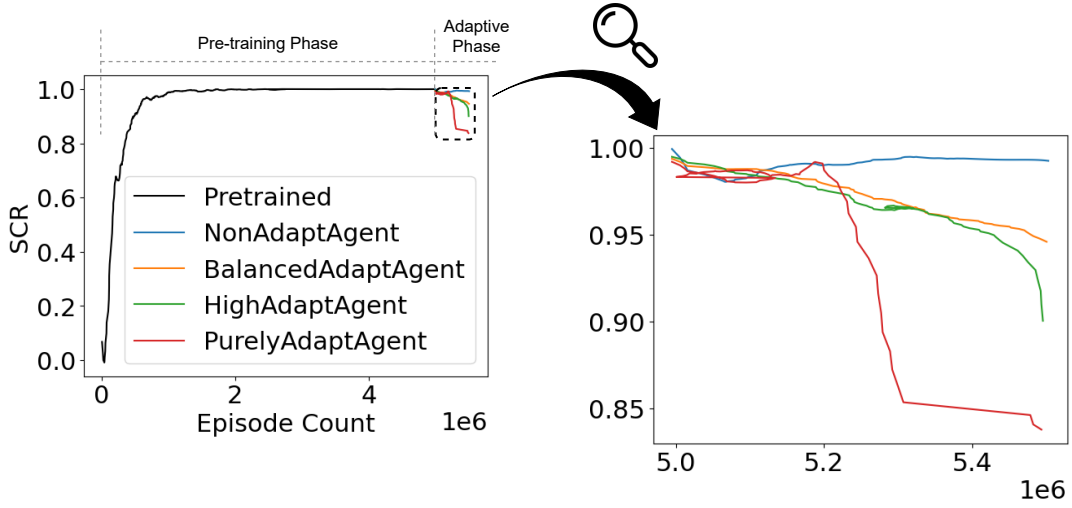


Fig. 5: *Surgery Completion Rate (SCR)* results for the complete training cycle of four agents with different strength factor ratios  $\lambda_{gail}$  and  $\lambda_{env}$  (see Table I).

TABLE II: AdSSR values for adaptive agents fine-tuned on surgeon demonstrations. Values correspond to the mean rate and standard error ( $AdSSR_{mean} \pm std_{err}$ ) at which the agent is able to follow their designated surgeon’s approach.

Surgeon Adaptation	NonAdaptAgent	BalancedAdaptAgent	HighAdaptAgent	PurelyAdaptAgent
Left (Any)	$0.28 \pm 0.002$	$0.28 \pm 0.002$	$0.44 \pm 0.007$	$0.70 \pm 0.012$
Left 1 (Upper)	$0.07 \pm 0.019$	$0.07 \pm 0.019$	$0.11 \pm 0.062$	$0.18 \pm 0.099$
Left 2 (Middle)	$0.11 \pm 0.014$	$0.12 \pm 0.014$	$0.18 \pm 0.040$	$0.28 \pm 0.070$
Left 3 (Lower)	$0.10 \pm 0.015$	$0.10 \pm 0.015$	$0.15 \pm 0.050$	$0.24 \pm 0.080$
Right (Any)	$0.72 \pm 0.001$	$0.72 \pm 0.001$	$0.80 \pm 0.010$	$0.84 \pm 0.011$
Right 1 (Upper)	$0.19 \pm 0.042$	$0.19 \pm 0.042$	$0.21 \pm 0.170$	$0.22 \pm 0.200$
Right 2 (Middle)	$0.30 \pm 0.038$	$0.30 \pm 0.034$	$0.33 \pm 0.160$	$0.35 \pm 0.180$
Right 3 (Lower)	$0.23 \pm 0.040$	$0.24 \pm 0.034$	$0.26 \pm 0.170$	$0.27 \pm 0.190$

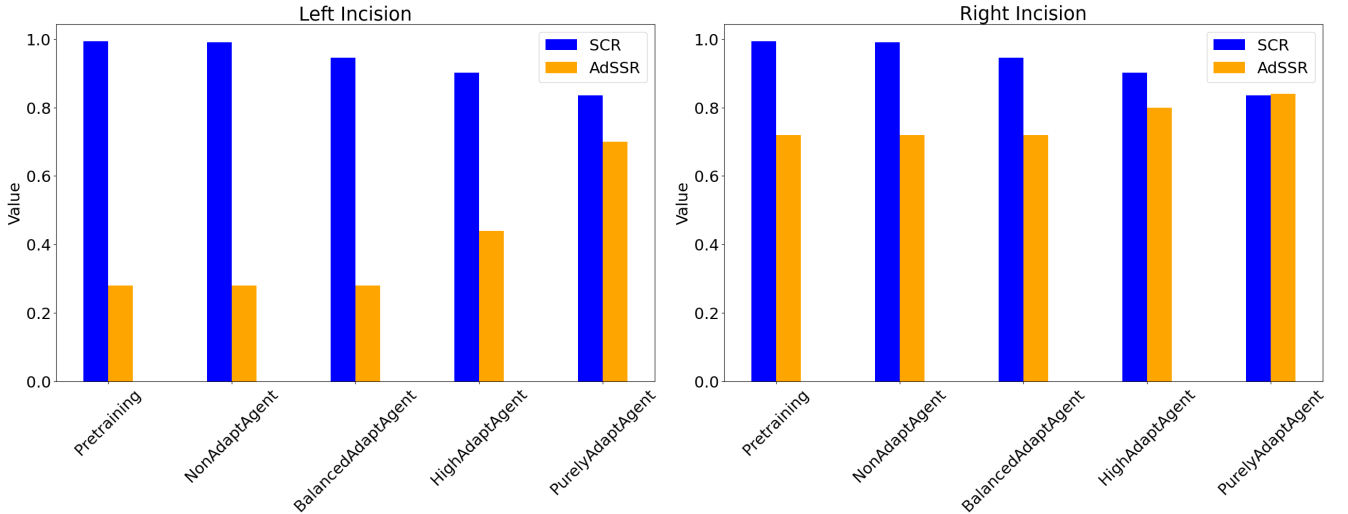


Fig. 6: Comparison between SCR and AdSSR metrics for left and right incision across all agents.

creating a single model capable of understanding and isolating various surgical approaches, responding to control input signals to switch between them as needed. This dynamic adaptability would enable autonomous surgical agents

to cater to different surgeons’ preferences and adapt to a variety of surgical scenarios. In summary, this research has contributed valuable insights and methodologies to the field of surgeon-centered autonomous surgical robotics. By

addressing the challenges of adaptability and precision, it paves the way for future advancements aimed at improving patient outcomes, reducing surgical errors, and improving the overall surgical experience.

## ACKNOWLEDGMENT

This work is partially funded by the German Ministry of Education and Research (BMBF) under the TeachTAM project (Grant Number: 01IS17043).

## REFERENCES

- [1] S. DiMaio, M. Hanuschik, and U. Kreaden, "The da vinci surgical system," in *Surgical robotics*. Springer, 2011, pp. 199–217.
- [2] I. Surgical, "The Da Vinci Surgical robot," 2022. [Online]. Available: <https://www.intuitive.com/en-us/about-us/company>
- [3] S. Datta, Y. Li, M. M. Ruppert, Y. Ren, B. Shickel, T. Ozrazgat-Baslanti, P. Rashidi, and A. Bihorac, "Reinforcement learning in surgery," *Surgery*, vol. 170, no. 1, pp. 329–332, 2021. [Online]. Available: <https://www.sciencedirect.com/science/article/pii/S0039606020308254>
- [4] F. Richter, R. K. Orosco, and M. C. Yip, "Open-sourced reinforcement learning environments for surgical robotics," 2019. [Online]. Available: <https://arxiv.org/abs/1903.02090>
- [5] A. T. Bourdillon, A. Garg, H. Wang, Y. J. Woo, M. Pavone, and J. Boyd, "Integration of reinforcement learning in a virtual robotic surgical simulation," *Surgical Innovation*, vol. 30, no. 1, pp. 94–102, 2023.
- [6] N. D. Nguyen, T. Nguyen, S. Nahavandi, A. Bhatti, and G. Guest, "Manipulating soft tissues by deep reinforcement learning for autonomous robotic surgery," in *2019 IEEE International Systems Conference (SysCon)*, 2019, pp. 1–7.
- [7] Y.-H. Su, K. Huang, and B. Hannaford, "Multicamera 3d viewpoint adjustment for robotic surgery via deep reinforcement learning," *Journal of Medical Robotics Research*, vol. 06, no. 01n02, p. 2140003, 2021. [Online]. Available: <https://doi.org/10.1142/S2424905X21400031>
- [8] Y. Barnoy, M. O'Brien, W. Wang, and G. Hager, "Robotic surgery with lean reinforcement learning," 2021. [Online]. Available: <https://arxiv.org/abs/2105.01006>
- [9] G. Ning, X. Zhang, and H. Liao, "Autonomic robotic ultrasound imaging system based on reinforcement learning," *IEEE Transactions on Biomedical Engineering*, vol. 68, no. 9, pp. 2787–2797, 2021.
- [10] D. Baek, M. Hwang, H. Kim, and D.-S. Kwon, "Path planning for automation of surgery robot based on probabilistic roadmap and reinforcement learning," in *2018 15th International Conference on Ubiquitous Robots (UR)*, 2018, pp. 342–347.
- [11] X. Gao, Y. Jin, Q. Dou, and P.-A. Heng, "Automatic gesture recognition in robot-assisted surgery with reinforcement learning and tree search," in *2020 IEEE International Conference on Robotics and Automation (ICRA)*, 2020, pp. 8440–8446.
- [12] J. Xu, B. Li, B. Lu, Y.-H. Liu, Q. Dou, and P.-A. Heng, "Surrol: An open-source reinforcement learning centered and dvrk compatible platform for surgical robot learning," in *2021 IEEE/RSJ International Conference on Intelligent Robots and Systems (IROS)*, 2021, pp. 1821–1828.
- [13] S. K. Pandey and V. Sharma, "Robotics and ophthalmology: Are we there yet?" *Indian J Ophthalmol*, vol. 67, no. 7, pp. 988–994, July 2019.
- [14] L. Torrey and J. Shavlik, "Transfer learning," in *Handbook of research on machine learning applications and trends: algorithms, methods, and techniques*. IGI global, 2010, pp. 242–264.
- [15] A. Gomaa, B. Mahdy, N. Kleer, M. Feld, F. Kirchner, and A. Krüger, "Teach me how to learn: A perspective review towards user-centered neuro-symbolic learning for robotic surgical systems," *arXiv preprint arXiv:2307.03853*, 2023.
- [16] E. H. Holly, "Mouth guide for operating microscope," *Journal of neurosurgery*, vol. 44, no. 5, pp. 642–643, 1976.
- [17] M. P. Sindou, *Practical handbook of neurosurgery*. Springer, 2009.
- [18] H. Afkari, S. Eivazi, R. Bednarik, and S. Mäkelä, "The potentials for hands-free interaction in micro-neurosurgery," in *Proceedings of the 8th Nordic Conference on Human-Computer Interaction: Fun, Fast, Foundational*, 2014, pp. 401–410.
- [19] L. P. Kaelbling, M. L. Littman, and A. W. Moore, "Reinforcement learning: A survey," *Journal of artificial intelligence research*, vol. 4, pp. 237–285, 1996.
- [20] B. Kiumarsi, K. G. Vamvoudakis, H. Modares, and F. L. Lewis, "Optimal and autonomous control using reinforcement learning: A survey," *IEEE transactions on neural networks and learning systems*, vol. 29, no. 6, pp. 2042–2062, 2017.
- [21] V. Mnih, K. Kavukcuoglu, D. Silver, A. Graves, I. Antonoglou, D. Wierstra, and M. Riedmiller, "Playing atari with deep reinforcement learning," 2013.
- [22] B. Jang, M. Kim, G. Harerimana, and J. W. Kim, "Q-learning algorithms: A comprehensive classification and applications," *IEEE Access*, vol. 7, pp. 133 653–133 667, 2019.
- [23] R. J. Williams, "Simple statistical gradient-following algorithms for connectionist reinforcement learning," *Machine Learning*, vol. 8, no. 3, pp. 229–256, May 1992. [Online]. Available: <https://doi.org/10.1007/BF00992696>
- [24] J. Schulman, F. Wolski, P. Dhariwal, A. Radford, and O. Klimov, "Proximal policy optimization algorithms," 2017.
- [25] B. Zheng, S. Verma, J. Zhou, I. Tsang, and F. Chen, "Imitation learning: Progress, taxonomies and challenges," 2022.
- [26] A. Gomaa and B. Mahdy, "Unveiling the role of expert guidance: A comparative analysis of user-centered imitation learning and traditional reinforcement learning," pp. 1–10, 2023.
- [27] B. Fang, S. Jia, D. Guo, M. Xu, S. Wen, and F. Sun, "Survey of imitation learning for robotic manipulation," *International Journal of Intelligent Robotics and Applications*, vol. 3, no. 4, pp. 362–369, 2019.
- [28] M. Lopes, F. S. Melo, and L. Montesano, "Affordance-based imitation learning in robots," in *2007 IEEE/RSJ international conference on intelligent robots and systems*. IEEE, 2007, pp. 1015–1021.
- [29] N. Ratliff, J. A. Bagnell, and S. S. Srinivasa, "Imitation learning for locomotion and manipulation," in *2007 7th IEEE-RAS International Conference on Humanoid Robots*. IEEE, 2007, pp. 392–397.
- [30] Y. Zhu, Z. Wang, J. Merel, A. Rusu, T. Erez, S. Cabi, S. Tunyasuvunakool, J. Kramár, R. Hadsell, N. de Freitas, et al., "Reinforcement and imitation learning for diverse visuomotor skills," *arXiv preprint arXiv:1802.09564*, 2018.
- [31] F. Codevilla, M. Müller, A. López, V. Koltun, and A. Dosovitskiy, "End-to-end driving via conditional imitation learning," in *2018 IEEE international conference on robotics and automation (ICRA)*. IEEE, 2018, pp. 4693–4700.
- [32] Y. Pan, C.-A. Cheng, K. Saigol, K. Lee, X. Yan, E. Theodorou, and B. Boots, "Agile autonomous driving using end-to-end deep imitation learning," *arXiv preprint arXiv:1709.07174*, 2017.
- [33] J. Zhang and K. Cho, "Query-efficient imitation learning for end-to-end autonomous driving," *arXiv preprint arXiv:1605.06450*, 2016.
- [34] R. P. Bhattacharyya, D. J. Phillips, B. Wulfe, J. Morton, A. Kuefler, and M. J. Kochenderfer, "Multi-agent imitation learning for driving simulation," in *2018 IEEE/RSJ International Conference on Intelligent Robots and Systems (IROS)*. IEEE, 2018, pp. 1534–1539.
- [35] F. Torabi, G. Warnell, and P. Stone, "Behavioral cloning from observation," in *Proceedings of the 27th International Joint Conference on Artificial Intelligence*, 2018, pp. 4950–4957.
- [36] S. Arora and P. Doshi, "A survey of inverse reinforcement learning: Challenges, methods and progress," 2020.
- [37] J. Ho and S. Ermon, "Generative adversarial imitation learning," *Advances in neural information processing systems*, vol. 29, pp. 4565–4573, 2016.
- [38] G. Davis, "The evolution of cataract surgery," *Missouri medicine*, vol. 113, no. 1, p. 58, 2016.
- [39] E. Nouvellon, P. Cuvillon, J. Ripart, and E. J. Viel, "Anaesthesia for cataract surgery," *Drugs & aging*, vol. 27, pp. 21–38, 2010.
- [40] L. Buratto, *Phacoemulsification: principles and techniques*. Slack Incorporated, 2003.
- [41] A. Coca, H. Estévez, C. Fernández, and G. Esteban, "Building 3d models for reconstructing a virtual cataract surgery haptic simulation," in *Proceedings of the First International Conference on Technological Ecosystem for Enhancing Multiculturality*, ser. TEEM '13. New York, NY, USA: Association for Computing Machinery, 2013, p. 43–48. [Online]. Available: <https://doi.org/10.1145/2536536.2536544>
- [42] E. Chan, O. A. Mahroo, and D. J. Spalton, "Complications of cataract surgery," *Clinical and Experimental Optometry*, vol. 93, no. 6, pp. 379–389, 2010.